Engineering Science & Technology
http://ojs.wiserpub.com/index.php/EST/

Research Article

Influence of Starch Powder on Compressive Strength and Microstructural Properties of Geopolymer Composite Materials Based on Metakaolin

Cedric M. Dieuhou[1], Hervé K. Tchakouté[1,2*], Alexis N. Kamlo[3], C. P. Nanseu-Njiki[1], Claus H. Rüscher[2]

[1]Laboratory of Electrochemistry Analytic and Materials Engineering, University of Yaounde I, Faculty of Science, Department of Inorganic Chemistry, P.O. Box 812, Yaounde, Cameroon
[2]Institute of Mineralogy, Leibniz University Hanover, Callinstrasse 3, D-30167 Hanover, Germany
[3]Department of Chemistry, Higher Teacher Training College, University of Yaounde I, 4124 Yaounde, P.O. Box 47, Cameroon
Email: hervetchakoute@gmail.com

Received: 31 October 2023; **Revised:** 20 January 2024; **Accepted:** 22 February 2024

Abstract: The main objective of the present study is the investigation of the behaviour of starch powder incorporated at different levels (0, 5, 10, 15, 20, 25, and 30 wt%) on the compressive strength and microstructural properties of metakaolin-based geopolymers. Sodium silicate with a molar ratio of SiO_2/Na_2O of 1.6 was used as the hardener, and standard metakaolin was used as the aluminosilicate source. The results showed that when metakaolin was replaced by starch from 0 to 15 wt%, the compressive strength increased from 36.50 to 64.12 MPa. When metakaolin was replaced by starch above 15 wt%, the compressive strength decreased from 64.12 to 29.43 MPa. That of the reference geopolymer material is 36.50 MPa. The infrared spectra of the geopolymer composites indicate that the Si-O-C bonds are formed. The thermal behaviour of geopolymer composites containing starch shows a mass loss at around 100 and 278 °C. The geopolymer material without starch only shows a loss of mass at around 100 °C. The micrographs of the geopolymer composite with 15% by weight of starch show that the matrix is more compact, more homogeneous, and denser than the one without starch. On the contrary, possibly due to a large amount of unreacted starch in its network, the micrographs of the geopolymer composite obtained after the incorporation of 30 wt% starch show a heterogeneous microstructure. It can be concluded that the suitable starch content for the synthesis of geopolymer composites would be around 15% by weight.

DOI: https://doi.org/10.37256/est.5220243846

Graphical Abstract :

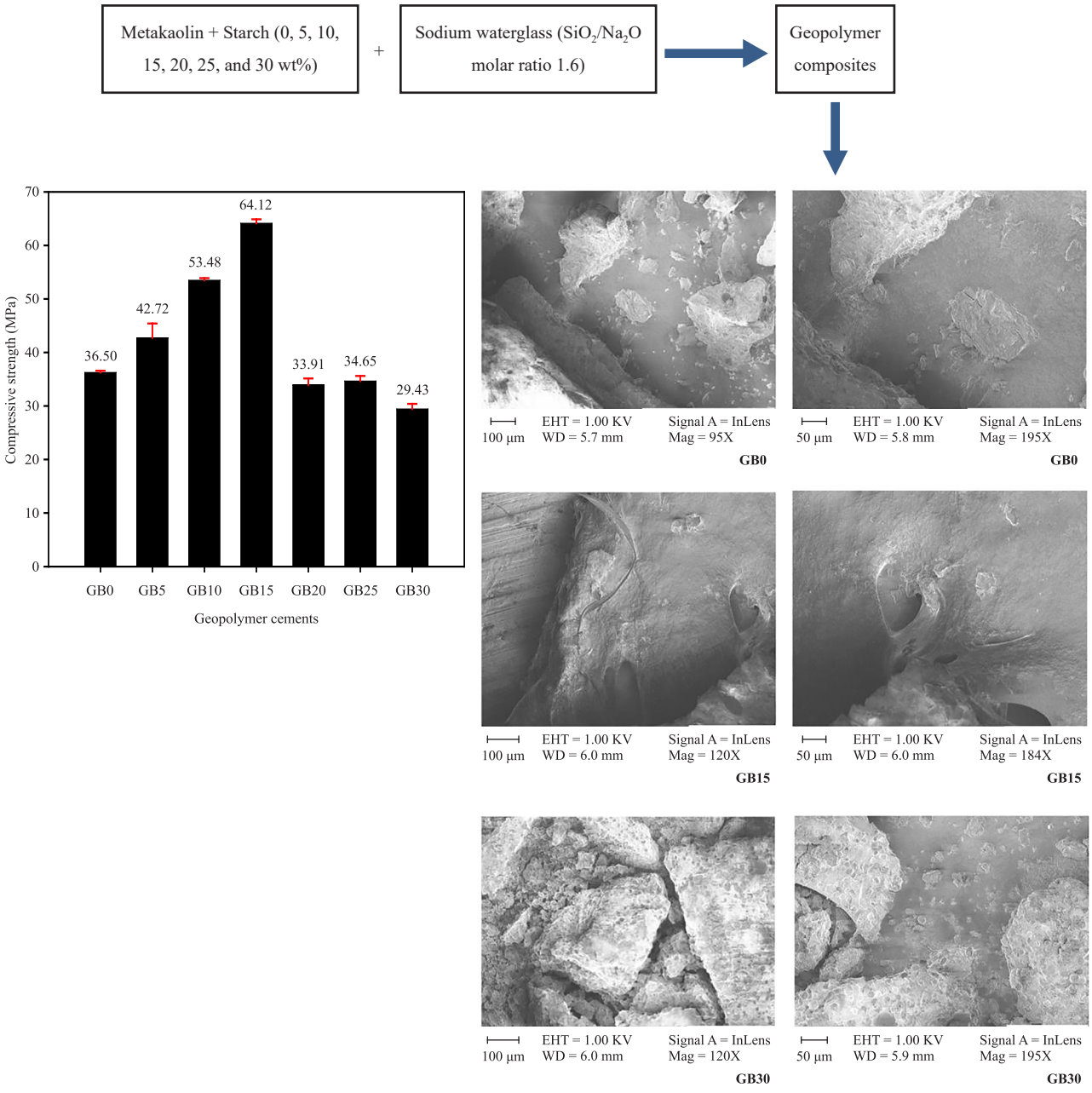

Keywords: starch, metakaolin, geopolymer composites, compressive strengths, microstructure, thermal behaviour

1. Introduction

Starch is a high molecular weight organic polymer derived directly from renewable plant sources and composed of two types of polysaccharides: amylose, a linear polymer, and amylopectin, a branched polymer [1], [2]. In this organic polymer, there are both crystalline and amorphous phases. According to Dome et al. [2], Sarko and Wu [3], Frost et al. [4], and Alay and Meireles [5], The crystalline part consists of double helices of amylopectin. The amorphous part is formed by amylose chains and branched segments of amylopectin. Amylose has a wide range of properties such as

thickening, water binding, emulsion stabilising, and gelling. Amylopectin has high starch content and is highly soluble [6]. Among these properties, it can be assumed that the water-binding and gelling agents can influence the properties of geopolymers. Many researchers have used starch as an additive to improve the properties of Portland cement-based concrete, such as Atia and Abbas [7] who studied the influence of biopolymer nano-starch on the properties of silica fume-based Portland concrete. The findings of these authors indicate an increase in compressive strength due to the greater cohesion and higher degree of polymerisation of the starch molecule. The presence of this organic polymer in Portland cement-based concrete leads to a more uniform microstructure. However, in the same vein, Akindahunsi and Uzoegbo [6] investigated the compressive strength and durability properties of Portland cement concrete using starch as an admixture. They concluded that the concrete with starch as an admixture had better compressive strength than the control concrete. In our view, the presence of starch in the structure of geopolymer materials could affect their properties, as in the case of Portland cement. This means that starch could also be used to improve the properties of geopolymer materials, as the reaction between starch and sodium silicate solution results in starch's enhanced properties such as thickener, water binder, emulsion stabiliser, and gelling agent [6]. With regard to the properties of gelling agents, Rashid et al. [8] have used a sodium silicate solution for the gelatinisation of starch. They reported that sodium silicate solution disrupts the molecular structure of starch and induces starch gelatinisation. In addition, the sodium silicate forms new C--O-O-SiO_2Na units with the starch component of the amylopectin. Other studies have been carried out using other organic compounds to investigate the influence of sodium tert-butoxide on the microstructure and strength of fly ash-based geopolymer materials [9]. They reported that the C-OH bonds in sodium tert-butoxide and Si-OH in the geopolymer structure can form C-O-Si bonds, which greatly improve the compressive strength and therefore contribute to the density of the microstructure. In contrast, the starch powder was used as a pore-forming agent in the preparation of porous geopolymer materials by Kaliappan et al. [10]. Geopolymer materials are the result of the mixing of an aluminosilicate source with a hardener. The hardener could be a solution of sodium silicate or potassium silicate and phosphoric acid, but the most commonly used hardener was a solution of sodium silicate. From our point of view, the reaction between the sodium water glass and the starch could play a decisive role in the properties of the geopolymer composites.

The effect of starch powder on the compressive strength of metakaolin-based geopolymer composites is the main objective of this work. The chemical reagent used is a commercially available sodium silicate glass. The molar ratio of SiO_2/Na_2O is 1.6. Metakaolin has been substituted by 0, 5, 10, 15, 20, 25, and 30 wt% of starch and the resulting powders have been used for the preparation of geopolymer composites. Compressive strength measurements were used to investigate the behaviour of starch in the structure of geopolymer composites. To identify the minerals present in the starch, metakaolin, and geopolymer composites, X-ray diffractometry was carried out. The functional groups were monitored by infrared spectroscopy and the morphologies of the geopolymer material fragments were studied by scanning electron microscopy.

2. Materials and experimental methods

2.1 *Materials*

The aluminosilicate source used was metakaolin (MK). Metakaolin is standard white kaolin supplied by BAL-CO of Modena, Italy. This company calcined white kaolin at 700 °C for 4 hours. It was commonly used in the production of glazed ceramic tiles. The chemical formula of the metakaolin obtained was as follows: $5{\cdot}4SiO_2{\cdot}4Al_2O_3$ [11]. Starch soluble with a loss on drying at 11 °C 4 mL containing sulphated ash of 0.5 wt% and chloride of 0.04 wt% was provided by a company called Kermel. Ingessil of Verona, Italy, provided the commercial sodium silicate solution with a molar ratio of SiO_2/Na_2O of 1.6.

2.2 *Experimental procedures*

2.2.1 *Synthesis of geopolymer composites*

Metakaolin was replaced by 0, 5, 10, 15, 20, 25, and 30 wt% of starch powder to produce geopolymer composites. To obtain the fresh geopolymer pastes, sodium silicate was gradually added to the obtained powder of each composition

and mixed for 5 minutes. The liquid/solid mass ratios were 0.83, 1.10, 1.19, 1.24, 1.28, 1.33, and 1.38 for geopolymer composites from the substitution of metakaolin by 0, 5, 10, 15, 20, 25, and 30 wt% of starch powder, respectively. The fresh paste of each formulation was poured into the 40 × 40 × 40 mm cube moulds. The moulds were cured for 24 hours in the laboratory before being demoulded. The demoulded specimens were sealed in the plastic for a period of 28 days at 27 ± 2 °C and 65% relative humidity. The geopolymer composites resulting from the replacement of metakaolin by 0, 5, 10, 15, 20, 25, and 30 wt% starch are designated GB0, GB5, GB10, GB15, GB20, GB25, and GB30, respectively. The mix design is shown in Table 1.

Table 1. Mix proportions of different geopolymer pastes

Metakaolin (g)	GB0 (g)	GB5 (g)	GB10 (g)	GB15 (g)	GB20 (g)	GB25 (g)	GB30 (g)	Hardener (g)	liquid-solid mass ratio (g)	Geopolymer materials
300	-	-	-	-	-	-	-	249.00	0.83	GB0
285	-	15	-	-	-	-	-	330	1.10	GB5
270	-	-	30	-	-	-	-	357	1.19	GB10
255	-	-	-	45	-	-	-	372	1.24	GB15
240	-	-	-	-	60	-	-	384	1.28	GB20
225	-	-	-	-	-	75	-	399	1.33	GB25
210	-	-	-	-	-	-	90	414	1.38	GB30

2.2.2 *Characterization methods of different starch and geopolymer composites*

For the determination of the major different oxides content in the metakaolin (MK), about 4.0 g of the metakaolin (MK) powder was added to about 0.9 g of Wax C micro powder (binder for XRF provided by Fluxana GmbH & Co. KG Borschelstrasse 3, 47,551-Belburg-Hau, Germany) and mixed for 20 minutes in a RETSCH MM 400 mixer mill at 10 Hz frequency. A hydraulic press (SPECAC) was used to compress the whole into a pellet at 166 kN. The resulting pellet was used to determine the major oxides present in the metakaolin using an XEPOS HE-146,615 from the AMETEK Materials Analysis Division. XRF Analyzer Pro software was used to determine the various major oxides.

The DIN 1,164 standard was used to measure the compressive strength of the metakaolin-based geopolymer composites after 28 days. This was carried out using a constant load rate of 0.500 MPa/s on a 250 kN capacity automatic hydraulic press (Impact Test Equipment Limited, UK KA20 3 LR). The selected samples of the fragments obtained were collected and one part was finely ground in the porcelain mortar and the other part was used to observe their morphology.

The X-ray pattern of each sample was registered on a Bruker D8 Advance equipped with a LynXeye XE-T detector detecting CuKα1,2 in Bragg-Brentano geometry with 2θ range covering between 5 and 80° for 2 h with 0.01 2θ steps. X'Pert HighScore Plus software was used to identify the crystalline phases.

Prior to recording the infrared spectra of the samples using the KBr method, the pellets were prepared by adding approximately 1 mg of each sample to approximately 200 mg of KBr. The whole was mixed in an agate mortar. It was then pressed at 100 kN using a hydraulic press (ENERPAC P392, USA). The pellet obtained from each sample was used to record a spectrum on the Bruker Vertex 80v with a resolution of 2 cm^{-1} and 16 scans and the data was collected using OPUS software.

TG and DSC analyses of the powders of the geopolymer composites GB0 and GB30 were carried out using an

alumina crucible between 25 and 1,000 °C (technical air with a flow rate of 20 mL/min, 10 °C/min heating/cooling rate, Setaram Setsys Evolution 1650).

The fragments obtained from the compressive strength measurements were used to determine the morphology of the metakaolin-based geopolymer composites. The structural morphology was characterised by scanning electron microscopy (SEM) using a ZEISS GEMINI 500 microscope coupled to an Oxford Instruments X-max detector, using an acceleration voltage of 1 kV for imaging. Without any additional conductive sputter coating, the samples were mounted on an aluminium stub fixed with carbon tape.

3. Results and discussion

3.1 *Characterization of starch and metakaolin*

3.1.1 *Chemical composition of metakaolin*

Table 2 shows the chemical composition of metakaolin (MK). This semi-crystalline aluminosilicate source has a high silica (58.31 wt%) and alumina (37.50 wt%) content associated with some impurities such as Fe_2O_3, TiO_2, K_2O, CaO, MgO, MnO, Na_2O, and ZrO_2. The small contribution of Fe_2O_3 (1.59 wt%) is due to trace iron minerals in metakaolin. The presence of anatase or rutile is indicated by the TiO_2 content (1.65 wt%). The presence of micaceous or K-feldspathic minerals may account for the presence of 0.8 wt% K_2O in the structure of metakaolin.

Table 2. Chemical composition of metakaolin (MK) in wt%

Oxides	SiO_2	Al_2O_3	Fe_2O_3	TiO_2	K_2O	MgO	CaO	MnO	ZrO_2	Na_2O
wt%	58.310	37.500	1.590	1.650	0.800	0.140	0.130	0.270	0.060	< 0.004

3.1.2 *X-ray patterns of starch and metakaolin*

The X-ray patterns of starch and metakaolin are depicted in Figure 1 and Figure 2, respectively. Crystalline peaks at 15.03, 19.82, and 23.02 and doublet peaks at 17.24 and 17.97° (2θ) are present in the X-ray pattern of starch. These peaks correspond to the A-type crystalline structure [12], [13]. According to Todica et al. [14], these crystalline peaks are ascribed to amylopectin. The amorphous phase called amylose is responsible for the broad hump structure located between 7 and 60° (2θ). Illite, anatase, and quartz peaks are seen in the diffractogram of metakaolin. The presence of the main anatase and illite peaks is consistent with the chemical composition (Table 1), which shows TiO_2 (1.65 wt%) and K_2O (0.8 wt%), respectively. The presence of trace amounts of this iron mineral is indicated by the absence of iron mineral peaks on the diffractogram of metakaolin. In addition to these crystalline phases, the X-ray pattern of metakaolin shows a broad hump structure ranging from 15 to 40° (2θ), corresponding to the presence of metakaolinite (amorphous aluminosilicate). The presence of crystalline peaks and amorphous phases in the structures of starch and metakaolin indicate that both raw materials are semi-crystalline materials.

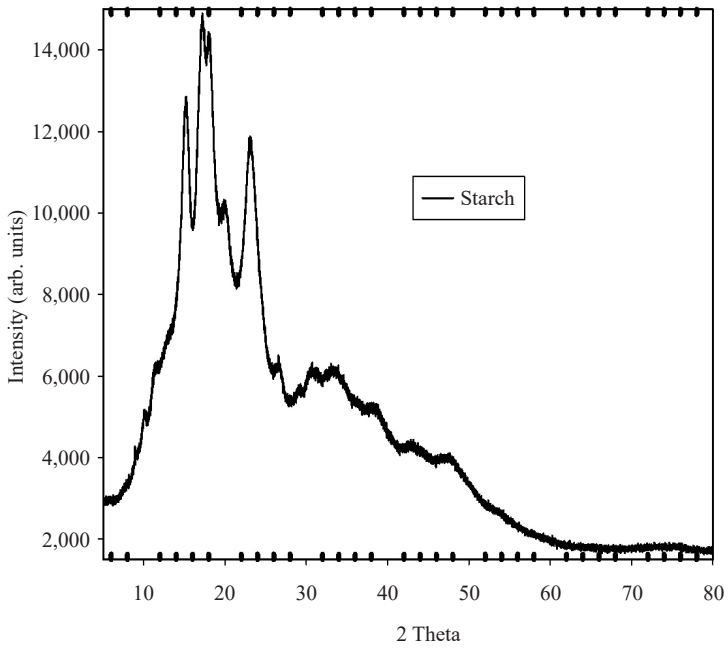

Figure 1. X-ray pattern of starch

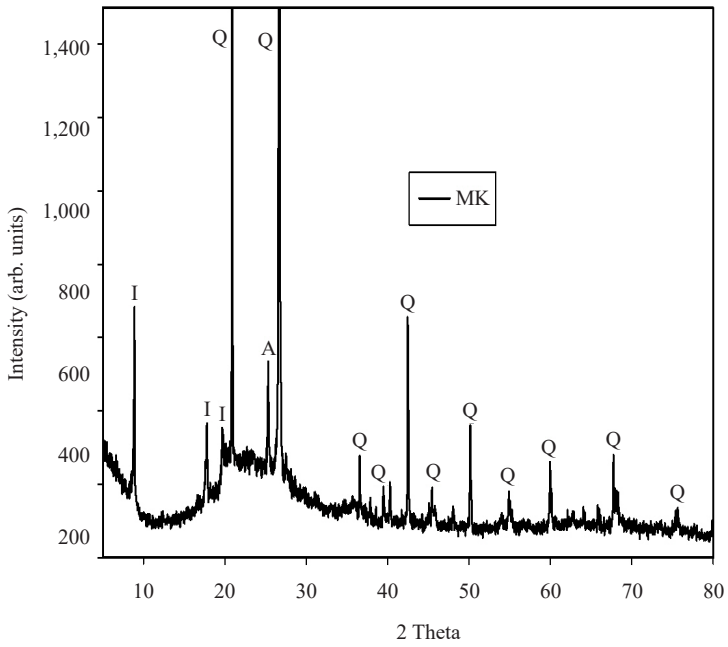

Figure 2. X-ray pattern of metakaolin. I, Q and A denote peaks of illite, quartz, and anatase, respectively

3.1.3 *Infrared spectra starch and metakaolin*

Figure 3 depicts the infrared spectra of starch and metakaolin. The O-H bending and stretching absorption bands at 1,643-1,636 and 3,550-3,401 cm^{-1}, respectively, are found in the spectra of starch and metakaolin. The starch spectrum

shows C-H stretching at 2,922 cm^{-1} [15]. There are also C-H bending absorption bands in the starch spectrum at 1,419 and 1,353 cm^{-1} [16]. According to Huang et al. [17] and Ogunmolasuyi et al. [18], the absorption bands located at 513, 567, 700, and 752 cm^{-1} on the spectrum of starch are attributed to the skeletal mode vibrations of the pyranose ring in the glucose unit. The absorption band located at 861 cm^{-1} in the spectrum of starch has been designed for the bending vibration modes of the C-H bond. The absorption band located at 989 cm^{-1} on the spectrum of starch belongs to the skeletal vibration modes of the α-1, 4 glycosidic linkage characteristic of polysaccharides [18]. The stretching vibration modes of the C-O and C-C bonds are assigned to the observed 1,143 cm^{-1} [18]. The absorption bands located at 472, 554, and 800 cm^{-1} on the spectrum of metakaolin correspond to the bending vibrations of Si-O-Si bonds, the stretching vibrations of Si-O-Al^{VI} bonds, and the stretching vibration modes of Si-O-Si of amorphous silica, respectively. The main band situated at 1,070 cm^{-1} on the spectrum of metakaolin is assigned to the symmetric and asymmetric stretching vibrations of Si-O-Si and Si-O-Al^{IV} bonds.

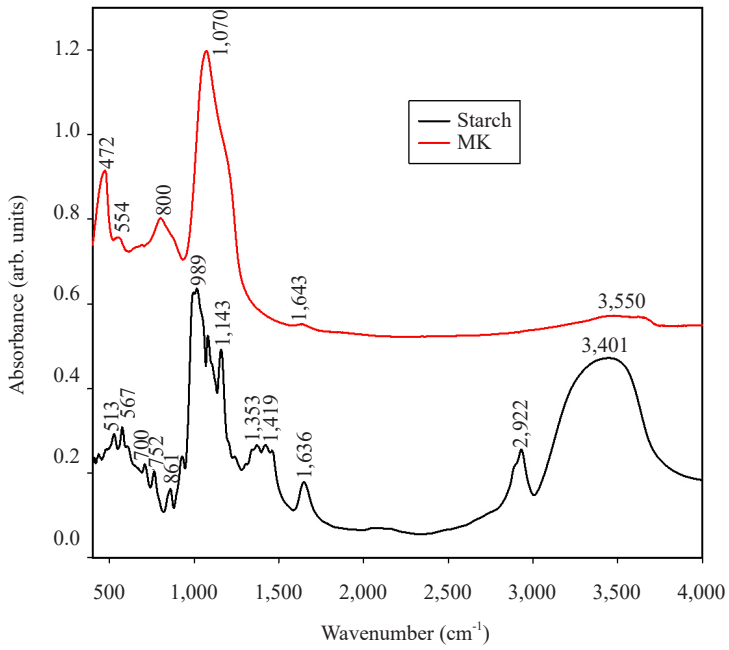

Figure 3. Infrared spectra of starch and metakaolin

3.2 *Characterization of geopolymer composites*

3.2.1 *X-ray patterns*

Figure 4 displays the X-ray patterns of the selected geopolymer composites, GB0, GB15, and GB30. The X-ray patterns of geopolymer composites reveal the crystalline minerals. These include illite, quartz, and anatase. The absence of amylose and amylopectin phase peaks in the X-ray patterns of GB15 and GB30 could be attributed to the incorporation of these phases into the structure of the final products, leading to the formation of C-O-Si-O-Si-O-C [19]. In addition to these crystalline phases, the X-ray patterns of the geopolymer composites depict the broad hump structure in the range 18-40° (2θ) belonging to the amorphous phase (binder) in the networks of the geopolymer composites. It is important to note that this broad hump structure is observed from 15 to 35° (2θ) on the X-ray pattern of metakaolin (Figure 2), indicating the change in microstructure due to the addition of sodium water glass and the incorporation of starch into the structure of metakaolin.

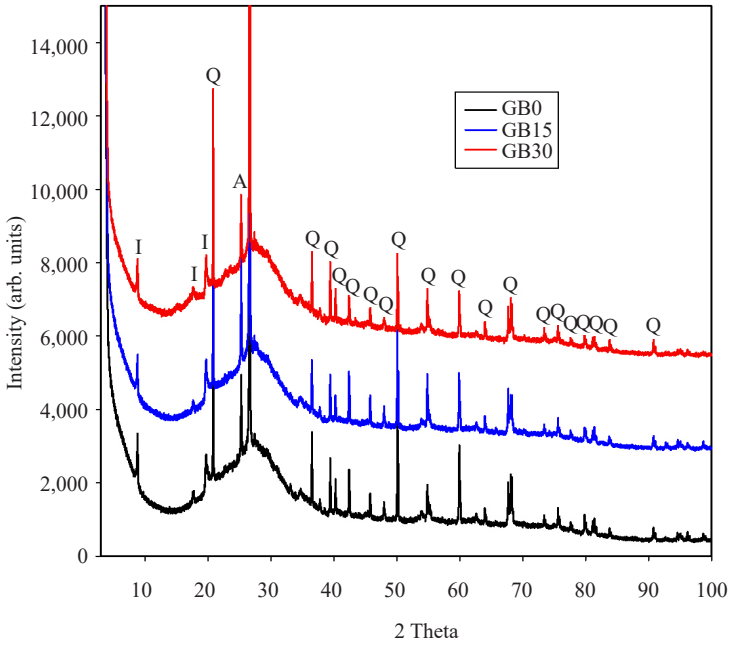

Figure 4. X-ray pattern of metakaolin-based geopolymer composites, GB0, GB15, and GB30. I, Q, and A denote peaks of illite, quartz, and anatase, respectively

3.2.2 *Infrared spectra*

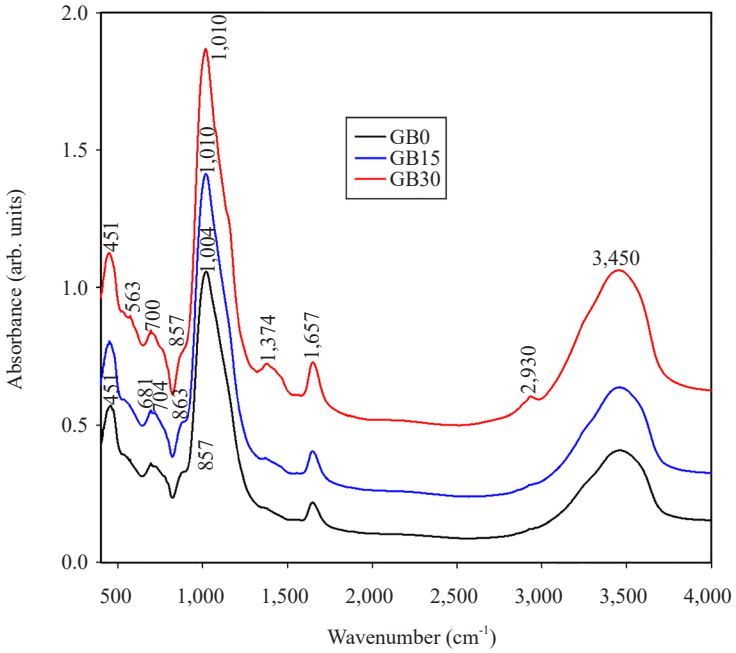

Figure 5. Infrared spectra of metakaolin-based geopolymer composites, GB0, GB15, and GB30

The infrared spectra of geopolymer composites, GB0, GB15, and GB30 are displayed in Figure 5. This figure

shows the broadband at about 3,450 cm^{-1} corresponding to the stretching vibration modes of O-H of Si-OH and Al-OH groups on the surface of geopolymer composites. The bending modes of H-O-H appear at around 1,657 cm^{-1}. The intensity of both adsorption bands is higher on the infrared spectrum of GB30 indicating that the geopolymer composites contain more silanol (Si-OH) groups and water in their structure. The presence of the absorption band between 863 and 857 cm^{-1} confirms the presence of the silanol groups. The lower degree of polycondensation reaction may be due to the higher content of silanol groups. The low degree of the polycondensation process is confirmed by the presence of the absorption band at 1,374 cm^{-1} which is assigned to the stretching band of the O-C-O bonds. The shoulder C-H stretching band is well visible at 2,922 cm^{-1}. It is observed on the infrared spectrum of geopolymer composites containing 30 wt% of starch. On the spectrum of GB15, the trace of this band is observed. The Si-O-Si bending modes are observed at 451 and 440 cm^{-1} on geopolymer composite spectra. A trace of a pyranose ring is observed at 563 cm^{-1} in GB30. The absorption band of quartz is observed at about 681 cm^{-1}. Associated with the formation of geopolymer materials, the stretching absorption band of sialate (Si-O-Al) bonds is observed at about 700 cm^{-1}. The stretching vibrations of the Si-O-C bonds could also be responsible for this broad band [20] and is an indication of the overlap bonds of Si-O-Al and Si-O-C. The reaction of starch with sodium water glass may be responsible for the formation of Si-O-C bonds.

3.2.3 *TG/DSC and dTG curves of metakaolin, geopolymer composites GB0 and GB30*

Figure 6 depicts the thermal stability of metakaolin and geopolymer composites (GB0 and GB30). They were investigated by thermogravimetric analysis (TG), differential scanning calorimetry (DSC), and the first derivative of TG (dTG). Thermal decomposition at 51, 133, and 97 °C is shown in the TG and dTG curves of metakaolin, GB0, and GB30, respectively. These endothermic peaks correspond to a significant weight loss on the TG curves of GB0 and GB30. A smaller weight loss is observed for MK. This includes large pore water evaporation in the structure of geopolymer composites and smaller evaporated water in metakaolin. This could be attributed to the difference between the microstructure of geopolymer composites and that of metakaolin, which supports the results of the X-ray patterns (displacement toward high broad hump structure: Figure 4) and infrared spectra (shift toward lower wavenumber of the main band: Figure 5). The weak endothermic peak observed on the DSC curve of metakaolin, which does not appear on its TG curve, results from the polymorphic transformation of α-quartz to β-quartz. An exothermic peak located at about 985 °C on the DSC curve of metakaolin belongs to the transformation of metakaolinite into a cubic Al-Si spinel phase [21]-[24], as can be seen from the following equation:

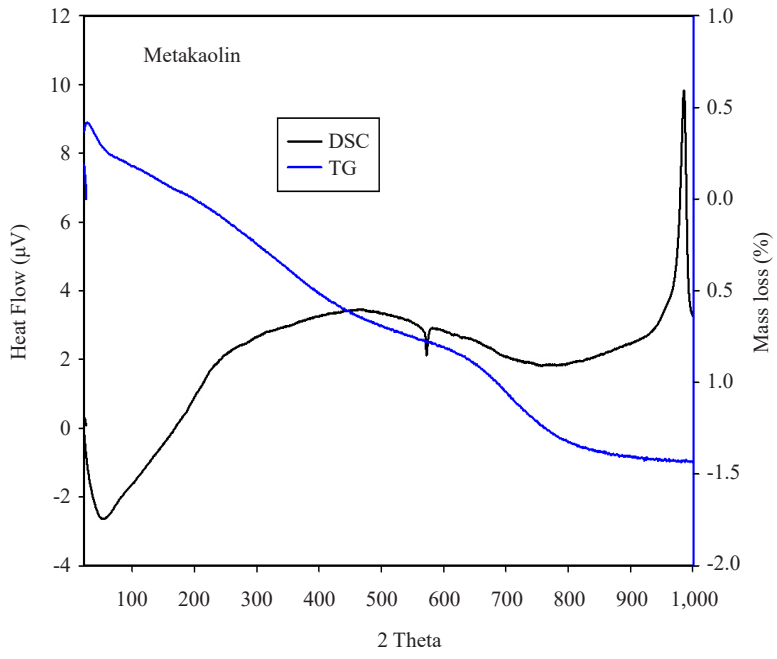

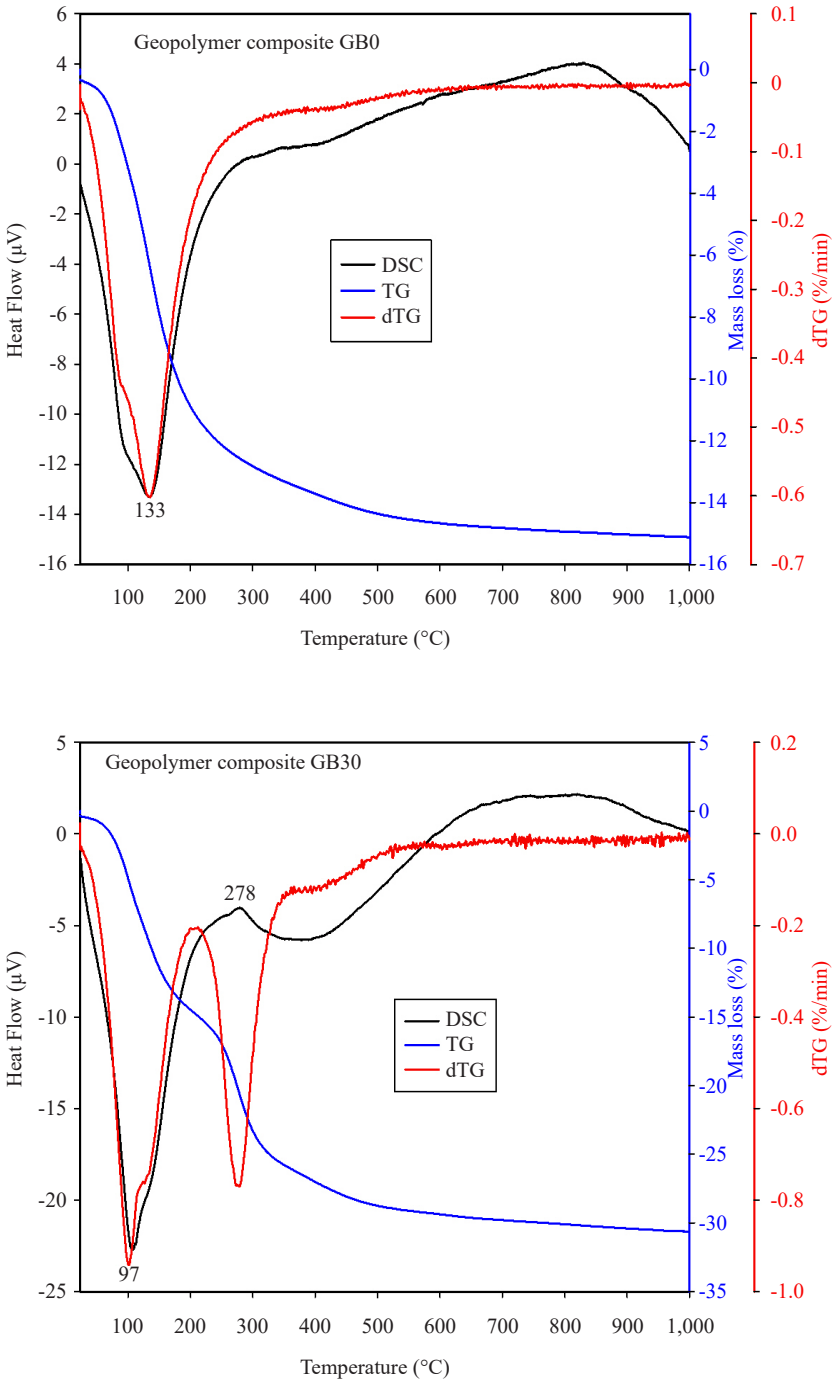

Figure 6. TG/DSC and dTG of metakaolin, geopolymer composites GB0 and GB30

$$2(Al_2O_3{\cdot}2SiO_2) \rightarrow 2Al_2O_3 \cdot 3SiO_2 + SiO_2$$

Metakaolinite (Al-Si spinel)

The mass loss between 150 and 300 °C on the TG curve of GB0 is attributed to the loss of intermolecular and crystalline water present in the structure of the geopolymer composite [25]-[27]. The loss of mass at around 278 °C on the TG and dTG curves is accompanied by the exothermic peak on the DSC curve of GB30, which belongs to the

decomposition of the starch [8] incorporated in the structure of the GB30 geopolymer composites. An additional mass loss observed between 300 and 700 °C is attributed to the dehydroxylation of Si-OH and Al-OH groups present in the geopolymer composites GB0 and GB30 [25]-[27], leading to the formation of siloxane bonds (Si-O-Si). The presence of these bands is consistent with the infrared spectra of geopolymer composites (Figure 5), which show absorption bands at 863-857 and 3,450 cm^{-1}.

3.2.4 *Compressive strengths*

The compressive strength values of the geopolymer composites GB0, GB5, GB10, GB15, GB20, GB25, and GB30 are depicted in Figure 7. From this figure, it can be seen that the geopolymer composites GB0, GB5, GB10, GB15, GB20, GB25, and GB30 are 36.50, 42.72, 53.48, 64.12, 33.91, 34.65, and 29.43 MPa, respectively. Compressive strength values increase with increasing starch content from 0 to 15 wt%, and above 15 wt% compressive strengths decrease progressively as the percentage of incorporated starch powder increases. The best value for the compressive strength of the geopolymer composite is obtained with a starch addition of 15% by weight. The increase in compressive strength of the geopolymer composites from 36.50 to 64.12 MPa could be explained by the increasing degree of polymerisation of the starch, which results in a greater cohesive force in the structure of the composites. The higher degree of polymerisation of starch has been the subject of a report by Swinkels [28]. The increase in compressive strength could also be related to the gelatinisation of starch with hardener, followed by the disruption of the crystalline phase (amylopectin) present in starch by interaction with this crystalline phase. Such interaction involves the silylation of starch, resulting in the formation of the C--O-O-SiO_2Na units on the C6 carbon of the pyranose ring in the structure of geopolymer composites. As shown by Rashid et al. [8]. The decrease in compressive strength from 64.12 to 29.43 MPa could be attributed to the non-gelatinisation of amylopectin due to its higher content in the structure of geopolymer composites. The maximum compressive strength value obtained in this work (64.12 MPa) is comparable to that (65.2 MPa) obtained by Kaze et al. [29] in which the metakaolin was replaced by 50 wt% calcined halloysite.

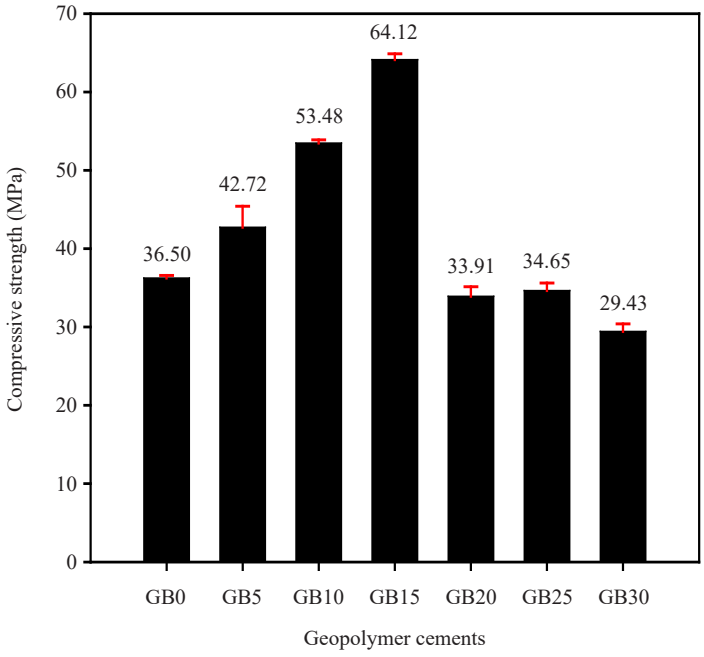

Figure 7. Compressive strengths of geopolymer composites GB0, GB5, GB10, GB15, GB20, GB25, and GB30

3.2.5 *Micrograph images*

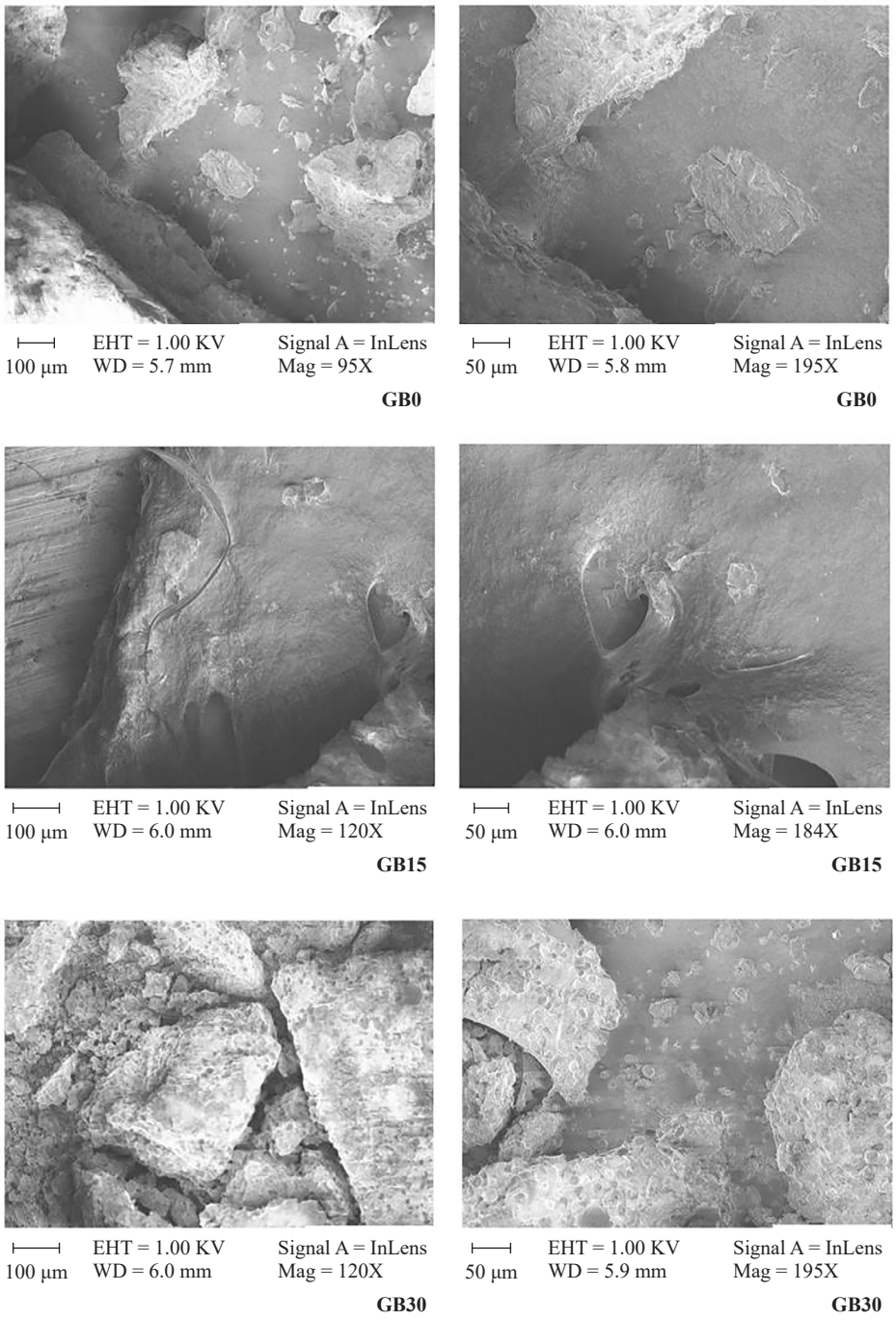

Figure 8. Micrograph images of geopolymer composites GB0, GB15, and GB30

The micrographs of the geopolymer composites before the addition of starch (GB0) and after the addition of starch (GB15 and GB30) were made with the scales at 50 and 100 µm and are shown in Figure 8. The micrographs of the GB0 and GB15 geopolymer composites show homogeneous microstructures due to their compact and denser matrix as a result of the formation of Si-O-C bonds in GB15. This is in line with the values for the compressive strength of GB0

(36.50 MPa) and GB15 (64.12 MPa). Furthermore, the morphologies of GB15 show a more uniform microstructure than GB0. The micrographs show that GB15 is denser than GB0 and this could be related to the reaction between the starch and the sodium silicate solution, known as gelatinisation, which facilitates the dissolution of the metakaolin and leads to the formation of more compact and dense matrices. On the contrary, the micrographs of the geopolymer composite obtained after the incorporation of 30 wt% starch show a heterogeneous microstructure, possibly due to a large amount of unreacted starch in the network of the geopolymer composite GB30.

4. Conclusion

For the synthesis of geopolymer composites using sodium water glass with a SiO_2/Na_2O molar ratio of 1.6 as a hardener, standard metakaolin was used as an aluminosilicate source and different starch contents (0, 5, 10, 15, 20, 25, and 30 wt%) were incorporated into this aluminosilicate source. The compressive strength of the geopolymer material without the addition of starch is 36.50 MPa. Those of the geopolymer composites with the addition of 5, 10, 15, 20, 25, and 30 wt% of starch are 42.72, 53.48, 64.12, 33.91, 34.65, and 29.43 MPa, respectively. Those obtained for geopolymer composites containing 5, 10, 15, 20, 25, and 30 wt% starch are 42.72, 53.48, 64.12, 33.91, 34.65, and 29.43 MPa, respectively. On the one hand, the geopolymer material without starch shows a loss of mass at around 100 °C. This can be attributed to the loss of large amounts of pore water. The morphologies of the geopolymer composites with the substitution of metakaolin by 15 wt% starch are compact, homogeneous, denser, and more uniform in microstructure compared to the reference. On the other hand, those with a starch content of 30% by weight have a heterogeneous microstructure due to the presence of undissolved starch in their structure. It was found that the amount of starch incorporated into the structure of geopolymer compounds to achieve better compressive strength was typically about 15% by weight.

Acknowledgement

Pr. Dr Hervé Tchakouté Kouamo gratefully acknowledges Alexander von Humboldt-Stiftung for financial support for this work under the grant N° KAM/1155741 GFHERMES-P.

Ethical approval

This article does not contain any studies with human participants performed by any of the authors.

Conflict of interest

The authors declare no competing financial interest.

References

[1] G. Balčiunas, S. Vejelis, S. Vaitkus, and A. Kairyte, "Physical properties and structure of composite made by using hemp hurds and different binding materials," *Procedia Engineering*, vol. 57, pp. 159-166, 2013.
[2] K. Dome, E. Podgorbunskikh, A. Bychkov, and O. Lomovsky, "Changes in the crystallinity degree of starch having different types of crystal structure after mechanical pre-treatment," *Polymers*, vol. 12, no. 3, pp. 641, 2020.
[3] A. Sarko, and C. H. Wu, "The crystal structure of A-, B- and C- Polymorphs of amylose and starch," *Starch*, vol. 30, no. 3, pp. 73-78, 1978.
[4] K. Frost, D. Kaminski, G. Kirwan, E. Lascaris, and R. Shanks, "Crystallinity and structure of starch using wide angle X-ray scattering," *Carbohydrate and Polymers*, vol. 78, no. 3, pp. 543-548, 2009.

[5] S. C. A. Alay, and M. A. A. Meireles, "Physicochemical properties, modifications and applications of starches from different botanical sources," *Food Science and Technology*, vol. 35, pp. 215-236, 2015.
[6] A. A. Akindahunsi, and H. C. Uzoegbo, "Strength and durability properties of concrete with starch admixture," *International Journal of Concrete Structure and Materials*, vol. 9, no. 3, pp. 323-335, 2015.
[7] S. M. Atia, and W. A. Abbas, "Effect of starch powder on behavior of silica fume biopolymer concrete," *Engineering Technology Journal*, vol. 39, no. 12, pp. 1797-1805, 2021.
[8] I. Rashid, M. H. Al Omari, S. A. Leharne, B. Z. Chowdhry, and A. Badwan, "Starch gelatinization using sodium silicate: FTIR, DSC, XRPD, and NMR studies," *Starch-Starke*, vol. 64, no. 9, pp. 713-728, 2012.
[9] C. Lu, Q. Wang, Y. Liu, T. Xue, Q. Yu, and S. Chen, "Influence of new organic alkali activators on microstructure and strength of fly ash geopolymer," *Ceramics International*, vol. 48, no. 9, pp. 12442-12449, 2022.
[10] S. K. Kaliappan, A. A. Siyal, Z. Man, M. Lay, and R. Shamsuddin, "Application of organic additives as pore forming agents for geopolymer composites," *International Journal of Innovative Technology and Exploring Engineering*, vol. 8, no. 5S, pp. 236-240, 2019.
[11] E. Kamseu, M. Cannio, E. Obonyo, F. Tobias, M. Chiara, V. Sglavo, and C. Leonelli, "Metakaolin-based inorganic polymer composite: Effects of fine aggregate composition and structure on porosity evolution, microstructure and mechanical properties," *Cement and Concrete Composites*, vol. 53, pp. 258-269, 2014.
[12] V. Singh, S. Z. Ali, R. Somashekar, and P. S. Mukherjee, "Nature of crystallinity in native and acid modified starches," *International Journal of Food Properties*, vol. 9, no. 4, pp. 845-854, 2006.
[13] L. A. Munoz, F. Pedreschi, A. Leiva, and J. M. Aguilera, "Loss of birefringence and swelling behavior in native starch granules: Microstructural and thermal properties," *Journal of Food Engineering*, vol. 152, pp. 65-71, 2015.
[14] M. Todica, E. M. Nagy, C. Niculaescu, O. Stan, N. Cioica, and C. V. Pop, "XRD investigation of some thermal degraded starch based materials," *Journal of Spectroscopy*, vol. 2016, pp. 9605312, 2016.
[15] S. C. Pang, S. K. Chin, S. H. Tay, and F. M. Tchong, "Starch-maleate-polyvinyl alcohol hydrogels with controllable swelling behaviors," *Carbohydrate Polymers*, vol. 84, no. 1, pp. 424-429, 2011.
[16] C. T. Vasques, S. C. Domenech, V. L. S. Severgnini, L. A. O. Belmonte, M. S. Soldi, P. L. M. Barreto, and V. Soldi, "Effect of thermal treatment on the stability and structure of maize starch cast films," *Starch-Stärke*, vol. 59, no. 3-4, pp. 161-170, 2007.
[17] C. B. Huang, R. Jeng, M. Sain, B. A. Saville, and M. Hubbes, "Production, characterization, and mechanical properties of starch modified ophiostoma SPP," *Bioresources*, vol. 1, no. 2, pp. 257-269, 2006.
[18] A. M. Ogunmolasuyi, E. C. Egwim, M. A. Adewoyin, and E. J. Nkop, "Physicochemical and structural characterization of yam starch modified by potassium dihydrogen phosphate treatment in aqueous glycerol," *Edorium Journal of Biotechnology*, vol. 2, pp. 6-14, 2016.
[19] H. Staroszczyk, "Microwave-assisted silication of potato starch," *Carbohydrate Polymers*, vol. 77, no. 3, pp. 506-515, 2016.
[20] T. Oh, and C. K. Choi, "Comparison between SiOC thin films fabricated by using plasma enhances chemical vapor deposition and SiO_2 thin films by using Fourier Transform Infrared Spectroscopy," *Journal of the Korean Physical Society*, vol. 56, no. 4, pp. 1150-1155, 2010.
[21] P. Ptáček, D. Kubátová, J. Havlica, J. Brandstetr, F. Soukal, and T. Opravil, "Isothermal kinetic analysis of the thermal decomposition of kaolinite: the thermogravimetric study," *Thermochimica Acta*, vol. 501, no. 1-2, pp. 24-29, 2010.
[22] P. Ptáček, F. Šoukal, T. Opravil, M. Noskova, J. Havlica, and J. Brandštetr, "The kinetics of Al-Si spinel phase crystallization from calcined kaolin," *Journal of Solid State Chemistry*, vol. 183, no. 11, pp. 2565-2569, 2010.
[23] S. Sperinck, P. Raiteri, N. Marks, and K. Wright, " Dehydroxylation of kaolinite to metakaolin-a molecular dynamics study," *Journal of Materials Chemistry*, vol. 21, no. 7, pp. 2118-2125, 2011.
[24] P. Ptáček, F. Šoukal, T. Opravil, J. Havlica, and J. Brandštetr, "Crystallization of spinel phase from metakaoline: the nonisothermal thermodilatometric CRH study," *Powder Technology*, vol. 243, no. 283, pp. 40-45, 2013.
[25] T. Alomayri, F. U. A. Shaikh, and I. M. Low, "Mechanical and thermal properties of ambient cured cotton fabric-reinforced fly ash-based geopolymer composites," *Ceramics International*, vol. 40, no. 9, pp. 14019-14028, 2014.
[26] M. A. Villaquiran-Caicedo, R. M. de Gutiérrez, S. Sulekar, C. Davis, and J. C. Nino, "Thermal properties of novel binary geopolymers based on metakaolin and alternative silica sources," *Applied Clay Science*, vol. 118, pp. 276-282, 2015.
[27] N. U. Auqui, H. Baykara, A. Rigail, M. H. Cornejo, and J. L. Villalba, "An investigation of the effect of migratory type corrosion inhibitor on mechanical properties of zeolite-based novel geopolymers," *Journal of Molecular Structure*, vol. 1146, pp. 814-820, 2017.
[28] J. J. Swinkels, "Composition and properties of commercial native starches," *Starch*, vol. 37, no. 1, pp. 1-5, 1985.

[29] C. R. Kaze, S. B. K. Jiofack, Ö. Cngiz, T. S. Alomayri, A. Adeyemi, and H. Rahier, “Reactivity and mechanical performance of geopolymer binders from metakaolin/meta-halloysite blends,” *Construction and Building Materials*, vol. 336, no. 9, pp. 127546, 2022.